

Thermal process of silica glass microchannels fabricated by femtosecond laser ablation

Xiaoyan Sun (孙小燕), Dongmei Cui (崔东妹), Youwang Hu (胡友旺)*,
Dongkai Chu (褚东凯), Guowei Chen (陈国炜), Jinlong Yu (余金龙),
Jianhang Zhou (周舰航), and Ji'an Duan (段吉安)

State Key Laboratory of High Performance Complex Manufacturing, College of Mechanical and Electrical Engineering,
Central South University, Changsha 410083, China

*Corresponding author: huyw@csu.edu.cn

Received June 5, 2018; accepted August 30, 2018; posted online September 21, 2018

In order to improve the morphology of microchannels fabricated by femtosecond laser ablation, the thermal process was introduced into the post-treatment processing. It was found that the thermal process cannot only decrease the roughness but also the width and depth of the microchannel. The change rates of width, depth, and roughness of the microchannel increase with processing temperature. When we prolong the time of constant temperature, the change rate of the width decreases at the beginning, and then it tends to be stable. However, the change rates of depth and roughness increase, and then they tend to be stable. In this Letter, we discuss the reasons of the above phenomena.

OCIS codes: 140.3390, 230.7380, 240.6700.
doi: 10.3788/COL201816.101402.

With the progress of science and technology and the improvement of the quality of life, people pay more attention to the pursuit of health. A microfluidic chip is an important device of health detection through the concept of lab-on-a-chip, which is revolutionizing fields such as biology and chemistry^[1,2]. The microfluidic channel is the basic structure of the chip. Fused silica glass provides the necessary guarantee of high sensitivity and high reliability of microfluidic chips, but what is more important is that it has high transmittance in the visible and ultraviolet bands, which is convenient for optical detection. Therefore, fused silica glass is the most ideal choice of building many chip lab systems^[3].

Although mature semiconductor technology can combine lithography and etching technology and machine various microchannels with various sizes and complex morphology based on glass and silicon materials^[4-7], it can only produce a two-dimensional structure and is difficult to fabricate three-dimensional channels directly. However, the femtosecond laser with ultrashort pulses and extremely high peak power provides a new method to machine silica glass. It can avoid the generation of residual stress and heat affected zone. What is more important is that the three-dimensional microstructures can be fabricated by femtosecond laser ablation or laser-assisted chemical etching directly, such as fiber sensors^[8,9].

People pay more attention to the production of microchannels with a high depth to diameter ratio, where techniques, such as the time domain shaping of a double pulse and control of the polarization state^[10,11], are applied. However, the roughness of the microchannel has great influence on the fluid wettability, and the study of the control of surface roughness is not enough. Yahng *et al.*

investigated the effect of substrate temperature on femtosecond laser micro-processing of silicon, stainless steel, and glass. They found that with the increase of substrate temperature, the roughness and the ablation efficiency decreased^[12]. Braun *et al.* researched the influence of the substrate and surrounding air temperatures on the laser ablation rates of 248 nm excimer laser irradiation of Pyralin polyimide. They have interpreted the decline in the ablation rate with the increasing of temperature by invoking a phonon excitation due to high substrate temperature^[13]. Several research groups investigated the effect of the substrate and surrounding temperature on laser ablation, however, their experiment temperature was below 800°C, and there was less understanding of the effect of the high-temperature thermal process on the microstructure surface of ultrafast laser ablation.

This Letter explores the improvement of high-temperature thermal post-treatment on the morphology of microchannels. The effects of laser power, temperature, and the incubation time on the morphology of microchannels processed by femtosecond laser ablation were investigated, respectively. Also, through the confocal laser scanning microscope (LCM) and scanning electron microscope (SEM) images, we discussed the underlying mechanism about the effect of temperature on the ablation results.

Figure 1 shows the diagram of the experimental setup. The laser beam (Spectra Physics, Inc., has a central wavelength of 800 nm, repetition rate of 1 kHz, and a pulse width of 120 fs) passes through a shutter and an attenuator, then was focused on the surface of fused silica glass (commercial glass) by a 10 times objective (NA = 0.25). The fused silica glass was cut into 10 mm × 10 mm × 1 mm pieces, and two sides were polished. The sample

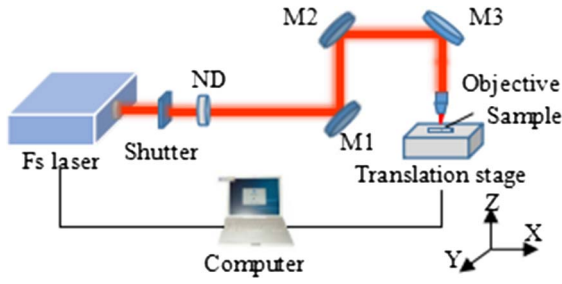


Fig. 1. Schematic diagram of the experimental setup. M, mirror; ND, neutral density attenuator.

is placed on a computer-controlled three-dimensional motion platform, as is shown in Fig. 1. The motion speed in the y direction is $100 \mu\text{m/s}$. The laser power is adjusted by a neutral density attenuator (ND). After processing is completed, the sample is treated with an ultrasonic bath for 15 min in distilled water. Then, the samples are heated by the KSY-6D-16 furnace. Finally, Carl Zeiss's LCM is employed to measure the morphology of microchannels.

Laser pulse power is one of the key factors affecting the morphology of the microchannel. The power used in our experiments is adjusted by an attenuator and ranges from 5 to 15 mW with the gradient of 2 mW. Figure 2(a) is the morphology of the microchannel, which is fabricated with 11 mW laser power, and Fig. 2(b) is the cross-section profile. The width, depth, and roughness of the microchannel can be obtained by the LCM. Analyzing the cross-section of the microchannel and selecting 10 positions to average, we can get the width and the depth of the channel as 16.6 and $18.3 \mu\text{m}$, respectively. The roughness is extracted from

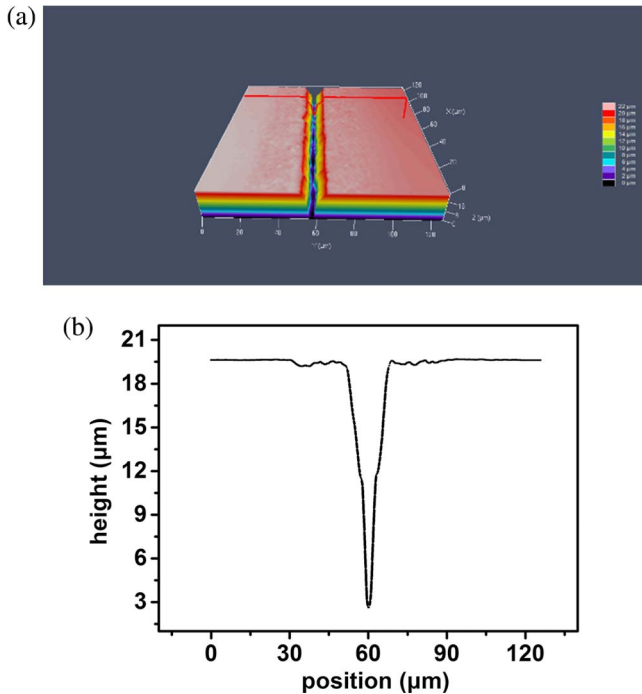


Fig. 2. (a) Morphology of the microchannel measured by the LCM; (b) cross-section profile.

the side wall in the depth direction near the upper position, and at least eight points are averaged to obtain the roughness. The roughness of the laser ablation surface of the microchannel is $0.9 \mu\text{m}$. Figure 3 shows the relationship between the morphology and the laser power at room temperature.

It can be seen from the Fig. 3(a) that the depth increases with the increase of laser power. However, the width of the microchannel increases at first and then becomes stable. When the laser power is low, only the light spot center produces ablation, and the radius of the ablation region is small. When the laser power is raised, the power density of the spot center goes up, which makes the region radius above the ablation threshold expand, and then the ablation area increases^[14]. However, when the laser power increases, the incident laser is scattered severely due to the change in the material structure of the focal region, resulting in the absorption of energy by the material being reduced^[15]. The reasons mentioned above result in the ablation width not being likely to expand continuously. The Rayleigh length is usually much larger than the waist radius, and with the power increase, the ablation depth is not easily saturated. Therefore, the depth increases continuously. The depth of the microchannel becomes larger with the power increase, leading to the ablated debris in microchannel being more difficult to get out. As a result, the roughness of the microchannel increases with the increase of laser power. Figure 3(b) shows the effects of laser power on roughness.

We design a microchannel where the width is $15 \mu\text{m}$, and the depth is $20 \mu\text{m}$. When the laser power is 15 mW, it can meet the requirement. Therefore, in the following experiment, the samples are processed by 15 mW laser power. However, the channel roughness is very large, above $1.6 \mu\text{m}$. In order to improve its morphology, we have adopted the method of heat treatment.

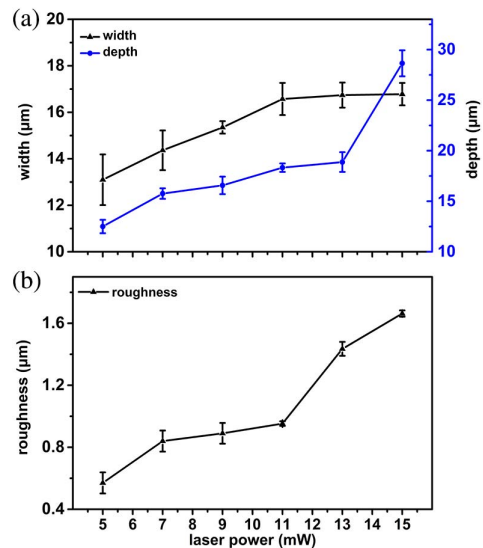


Fig. 3. Relationship between the morphology and the laser power.

We heat the sample from room temperature to 800°C with the temperature gradient of 200°C. When the heating furnace reaches the set temperature, it will be kept for 1 h and then cooled in the air naturally. Figure 4 reveals the relationship between the microchannel morphology and temperature.

With the increasing post-treatment temperature, the width, depth, and roughness of the microchannel are decreased, and the change rate of all of the parameters increases. Before laser processing, there are numerous SiO₄ tetrahedral cross-connections, which consist of a continuous network inside fused silica glass. The atom is long-range disordered, surrounded by a closed loop, which contains countless end-to-end Si–O bonds, which leads to the formation of numerous irregular N ring structures. N is the number of Si–O bonds in a closed loop. According to the shortest path analysis, the range of N is determined to be 3 to 9^[16], of which the six rings structure is the most stable one. Meanwhile, its number is also the largest. However, after laser irradiation, the relative number of the three rings or four rings structures of the irradiated area increased, and the number of other types reduced^[17]. The Si–O bond length of the 3 or 4 rings is not significantly different from that of the average value, however, the Si–O–Si bond angle of bridging obviously decreases, which results in the microstructure of laser irradiation area being unstable and varying with temperature^[18].

The surface of the channel fabricated by femtosecond laser ablation consists of 3 or 4 rings. When the temperature raises, the Si–O–Si bond angle of the fused silica glass decreases, resulting in reduction of tetrahedron volume, which makes the structure denser. However, in this experiment, the width and the depth of the surface channel reduced at the same time. The post-treatment temperature is much lower than that of femtosecond laser

ablation. Therefore, the Si–O–Si bond angle of the low bond angle structure of the ablation channel will not decrease with the increase of temperature, but increase instead, resulting in the volume of the surface material increasing with temperature, and the depth and the width of microchannel decreasing. The higher the temperature, the greater the influence on the Si–O–Si bond angle, leading to the change rate increase with the temperature.

When fused silica glass is heated, the surface melts at the beginning. The drop of viscosity results in viscous flow, which can partially repair the micro-defects. The specific surface area of the microchannel is large, and the proportion of the surface atoms is larger than the unprocessed area, since after the laser irradiation, the structure of three rings in the microchannel increased, whose most adjacent atoms are less than those in the internal six rings structure. The binding force is weaker, and the thermal motion of the atom is less constrained, therefore, the unflattened surface in the microchannel can be melted at a lower temperature^[19]. The effect of thermodynamics plays an important role in reducing the roughness. According to the thermodynamic size effect, the size of the microstructure in the channel surface decreases with the increase of temperature. This results in the roughness decrease with the increase of temperature. To further study the effect of temperature on roughness, a scanning electron microscope measurement is carried out, as is shown in Fig. 5. Figures 5(a) to 5(c) are the samples processed with room temperature, 400°C and 800°C, respectively. In each picture, we have selected an 80 × 80 rectangle and set the default threshold to statistics of the number of particles. The numbers of particles are 93, 112, and 145, respectively. The statistical results further prove that the particles in the microchannel become smaller after high-temperature thermal process.

Then, we further explored the influence of the incubation time on the microchannel morphology. According to Fig. 4, the change rate of the machined work piece is the largest at 800°C. Therefore, the work piece was heated to 800°C and then kept for different durations (1, 2, 3, 4, and 8 h, respectively). Figure 6 shows the change rate of the microchannel morphology with the incubation time.

It can be seen that with the increase of the incubation time, the change rate of width decreases at the beginning, and then it tends to be stable. While the change rates of depth and roughness increase, they tend to be stable. It is obvious that with the prolongation of the constant temperature, the volume of the microchannel decreases and tends to be stable, and the roughness is reduced and tends to be stable. The thermal expansion coefficient of fused silica glass is very small, and it needs enough time to transmit the temperature of the resistance box to that of the glass itself. Therefore, with the prolongation of the constant temperature, there is uniform heating of the glass, and it can be understood as equivalent to the increase of temperature. Due to the size effect of thermodynamics, a micro-melting zone exists in the microchannel structure,

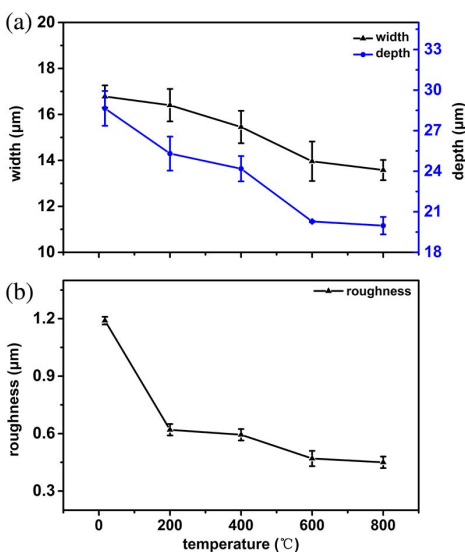


Fig. 4. Trend of width, depth, and roughness of microchannels varies with the temperature.

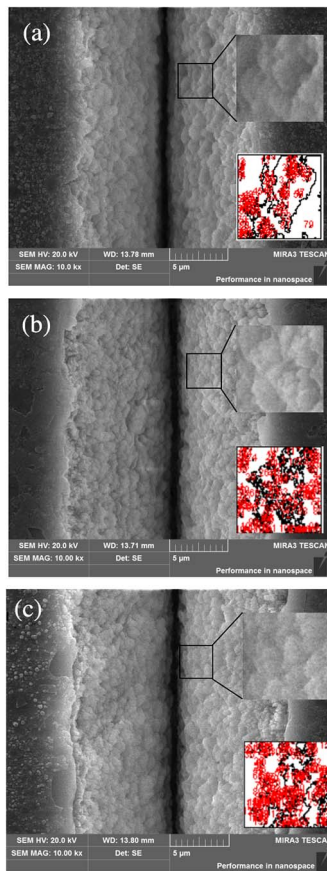


Fig. 5. SEM images of 15 mW heating at different temperatures and at an incubation time for 1 h. (a) Room temperature; (b) 400°C; (c) 800°C; the upper right corner is the selected area, and the lower right corner is the counting result.

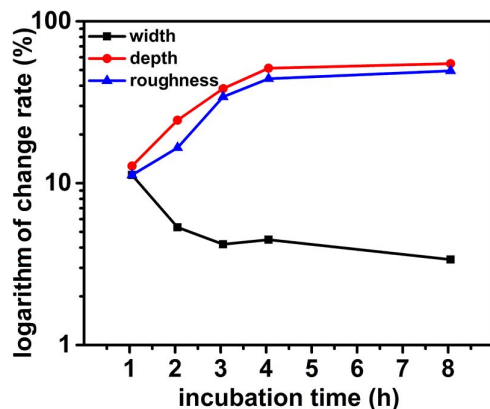


Fig. 6. Relationship between the change rate of the morphology and the incubation time when the work piece is heated to 800°C.

which results in particles becoming smaller and denser, and therefore, the roughness decreases with the incubation time. The surface tension increases with the rise of temperature. As a result, the depth of the microchannel gets shallower as time goes on, but there is no surface tension in the width direction of the microchannel, and thereby, the variation in the width direction is not obvious. The result of the comprehensive effect is that the volume of the

microchannel gets smaller and smaller until it reaches a stable state.

To sum up, in order to improve the roughness of the microchannel processed by a femtosecond laser, we have carried out some experiments on high-temperature annealing. The effects of different power, temperature, and thermostat time on the microchannel morphology were investigated. The experimental results show that the depth, width, and roughness of the microchannel will decrease with the increase of temperature. This is due to the fact that the Si–O–Si bond angle of the femtosecond laser ablation microchannel increases with processing temperature, resulting in an increase in the volume of the surface material as the temperature increases and a decrease in the size of the microchannel. The width and depth of the microchannel decrease. Due to the size effect of thermodynamics, the structure of the microchannel is not stable, and it can melt at a relatively low temperature. There the micro-melting zone may exist, which leads to the decrease of roughness. Because of the existence of surface tension, with the extension of constant temperature, the depth of the microchannel will be shallower until it reaches a stable state. At the same time, the volume of the microchannel is the smallest. In order to obtain a much lower surface roughness, the thermal process temperature should be higher, and for the processing temperature of 800°C, 4 h of incubation time is an optimized parameter.

This work was supported by the National Natural Science Foundation of China (Nos. 51475482, 51475482, 51475481, and 51875585) and the National Key R&D Program of China (Nos. 2018YFB1107803 and 2017YFB1104800).

References

1. G. M. Whitesides, *Nature* **442**, 368 (2006).
2. A. J. Demello, *Nature* **442**, 394 (2006).
3. Y. Bellouard, A. Said, M. Dugan, and P. Bado, *Opt. Express* **12**, 2120 (2004).
4. S. Wang, K. Liu, J. Liu, Z. T. F. Yu, X. Xu, L. Zhao, T. Lee, E. K. Lee, J. Reiss, and Y. K. Lee, *Angew. Chem. Int. Ed. Engl.* **123**, 3084 (2011).
5. H. Cheng, C. Han, Z. Xu, J. Liu, and Y. Wang, *Food Anal. Method* **7**, 2153 (2014).
6. T. Wienhold, S. Kraemmer, S. F. Wondimu, T. Siegle, U. Bog, U. Weinzierl, S. Schmidt, H. Becker, H. Kalt, and T. Mappes, *Lab Chip* **15**, 3800 (2015).
7. V. Murlidhar, M. Zeinali, S. Grabauskiene, M. Ghannadrezai, M. S. Wicha, D. M. Simeone, N. Ramnath, R. M. Reddy, and S. Nagrath, *Small* **10**, 4895 (2015).
8. X. R. Dong, X. Y. Sun, D. K. Chu, K. Yin, Z. Luo, C. Zhou, C. Wang, Y. W. Hu, and J. A. Duan, *IEEE Photon. Tech. Lett.* **28**, 2285 (2016).
9. X. Y. Sun, X. R. Dong, Y. W. Hu, H. T. Li, D. K. Chu, J. Y. Zhou, C. Wang, and J. A. Duan, *Sens. Actuators A Phys.* **230**, 111 (2015).
10. D. K. Chu, X. Y. Sun, Y. W. Hu, X. R. Dong, K. Yin, Z. Luo, J. Y. Zhou, C. Wang, and J. A. Duan, *Chin. Opt. Lett.* **15**, 071403 (2017).

11. D. K. Chu, X. Y. Sun, X. R. Dong, K. Yin, Z. Luo, G. W. Chen, J. A. Duan, Y. W. Hu, and X. Y. Zhao, *J. Phys. D Appl. Phys.* **50**, 46 (2017).
12. J. S. Yahng, J. R. Nam, and S. C. Jeoung, *Opt. Laser. Eng.* **47**, 815 (2009).
13. A. Braun, K. Zimmer, and F. Bigl, *Appl. Surf. Sci.* **154–155**, 73 (2000).
14. L. Y. Yao, “Femtosecond laser ablation mechanism and morphology characteristics of quartz glass” MA.Sc. Thesis, Dalian University of Technology, Dalian, China (2014).
15. G. H. Cheng, Q. Liu, L. Z. Yang, Y. S. Wang, S. F. Dong, W. Zhao, and G. F. Chen, *Acta Photon. Sin.* **32**, 1281 (2003).
16. A. Pasquarello and R. Car, *Phys. Rev. Lett.* **80**, 5145 (1998).
17. J. W. Chan, T. Huser, S. Risbud, and D. M. Krol, *Opt. Lett.* **26**, 1726 (2001).
18. Y. Ding, *Rare Metal. Mat. Eng.* **36**, 331 (2007).
19. J. L. Cui, L. J. Yang, and Y. Wang, *Rare Metal. Mat. Eng.* **43**, 369 (2014).